

Published in final edited form as:

*Nat Med.* 2008 December ; 14(12): 1363–1369. doi:10.1038/nm.1888.

## BMP type I receptor inhibition reduces heterotopic ossification

Paul B Yu<sup>1,2</sup>, Donna Y Deng<sup>1</sup>, Carol S Lai<sup>1</sup>, Charles C Hong<sup>3</sup>, Gregory D Cuny<sup>4</sup>, Mary L Boussein<sup>5</sup>, Deborah W Hong<sup>1</sup>, Patrick M McManus<sup>1</sup>, Takenobu Katagiri<sup>6</sup>, Chetana Sachidanandan<sup>1</sup>, Nobuhiro Kamiya<sup>7</sup>, Tomokazu Fukuda<sup>7</sup>, Yuji Mishina<sup>7,8,9</sup>, Randall T Peterson<sup>1,9</sup>, and Kenneth D Bloch<sup>1,2</sup>

<sup>1</sup> Division of Cardiology, Department of Medicine, Massachusetts General Hospital and Harvard Medical School, Thier 505, 50 Blossom Street, Boston, Massachusetts 02114, USA

<sup>2</sup> Anesthesia Centre for Critical Care Research, Massachusetts General Hospital and Harvard Medical School, Thier 505, 50 Blossom Street, Boston, Massachusetts 02114, USA

<sup>3</sup> Division of Cardiovascular Medicine and Department of Pharmacology, Vanderbilt University School of Medicine, 2220 Pierce Avenue, Nashville, Tennessee 37232, USA

<sup>4</sup> Laboratory for Drug Discovery in Neurodegeneration, Harvard NeuroDiscovery Center, Brigham & Women's Hospital and Harvard Medical School, 65 Landsdowne Street, Cambridge, Massachusetts 02139, USA

<sup>5</sup> Orthopedic Biomechanics Laboratory, Beth Israel Deaconess Medical Center and Harvard Medical School, 330 Brookline Avenue, Boston, Massachusetts 02215, USA

<sup>6</sup> Division of Pathophysiology, Research Center for Genomic Medicine, Saitama Medical University, 1397-1 Yamane, Hidakashi, Saitama 350-1241, Japan

<sup>7</sup> Molecular Developmental Biology Section, Laboratory of Reproductive and Developmental Toxicology, National Institute of Environmental Health Sciences, National Institutes of Health, 111 T.W. Alexander Road, Research Triangle Park, North Carolina 27709, USA

### Abstract

Fibrodysplasia ossificans progressiva (FOP) is a congenital disorder of progressive and widespread postnatal ossification of soft tissues<sup>1–4</sup> and is without known effective treatments. Affected individuals harbor conserved mutations in the *ACVRI* gene that are thought to cause constitutive activation of the bone morphogenetic protein (BMP) type I receptor, activin receptor-like kinase-2 (ALK2)<sup>5</sup>. Here we show that intramuscular expression in the mouse of an inducible transgene encoding constitutively active ALK2 (caALK2), resulting from a glutamine to aspartic acid change at amino acid position 207, leads to ectopic endochondral bone formation, joint fusion and functional impairment, thus phenocopying key aspects of human FOP. A selective inhibitor of BMP type I

Correspondence should be addressed to P.B.Y. (pbyu@partners.org).

<sup>8</sup>Present address: Department of Biologic and Materials Sciences, School of Dentistry, University of Michigan, 4222A Dental, 1011 North University Avenue, Ann Arbor, Michigan 48109, USA.

<sup>9</sup>These authors contributed equally to this work.

Note: Supplementary information is available on the Nature Medicine website.

#### AUTHOR CONTRIBUTIONS

P.B.Y. wrote the manuscript. P.B.Y., D.Y.D. and C.S.L. designed and performed experiments and analyzed data. G.D.C., P.B.Y., K.D.B. and R.T.P. helped to design, synthesize and evaluate dorsomorphin derivatives, and G.D.C. provided pharmacokinetic data. M.L.B. provided technical expertise and  $\mu$ CT tomography data. D.W.H. and P.M.M. performed experiments. C.S. tested the efficacy of the dorsomorphin derivative with additional assays. N.K. performed control experiments. Y.M. and T.F. provided key experimental reagents. T.K. provided reagents and experimental advice. C.C.H., Y.M. and K.D.B. provided feedback and experimental advice, and P.B.Y. and K.D.B. edited the manuscript.

Reprints and permissions information is available online at <http://npg.nature.com/reprintsandpermissions/>

receptor kinases, LDN-193189 (ref. 6), inhibits activation of the BMP signaling effectors SMAD1, SMAD5 and SMAD8 in tissues expressing caALK2 induced by adenovirus specifying Cre (Ad.Cre). This treatment resulted in a reduction in ectopic ossification and functional impairment. In contrast to localized induction of caALK2 by Ad.Cre (which entails inflammation), global postnatal expression of caALK2 (induced without the use of Ad.Cre and thus without inflammation) does not lead to ectopic ossification. However, if in this context an inflammatory stimulus was provided with a control adenovirus, ectopic bone formation was induced. Like LDN-193189, corticosteroid treatment inhibits ossification in Ad.Cre-injected mutant mice, suggesting caALK2 expression and an inflammatory milieu are both required for the development of ectopic ossification in this model. These results support the role of dysregulated ALK2 kinase activity in the pathogenesis of FOP and suggest that small molecule inhibition of BMP type I receptor activity may be useful in treating FOP and heterotopic ossification syndromes associated with excessive BMP signaling.

Individuals with FOP typically present within the first decade of life with progressive ectopic calcification of muscles and connective tissues after physical trauma, surgery, viral illness or myositis<sup>1-4</sup>. FOP results in severe debilitation and reduced life expectancy due to joint fusion and restrictive lung disease with thoracic involvement. A recent linkage and sequencing analysis identified heterozygous mutations in *ACVRI*, the gene encoding the BMP type I receptor ALK2, in all affected members from seven families<sup>5,7</sup>. BMP ligands facilitate the phosphorylation and activation of BMP type I receptors (ALK2, ALK3 and ALK6) by BMP type II receptors (BMPRII, ActRIIA and ActRIIB). Activated BMP type I receptors phosphorylate BMP-responsive SMAD1, SMAD5 and SMAD8, which translocate to the nucleus to regulate the transcription of genes, including the Inhibitor of DNA binding (*ID*) gene family, with broad effects on growth and differentiation<sup>8</sup>. The classic FOP-associated ALK2 mutation, R206H, is predicted to disrupt an  $\alpha$ -helix in the glycine-serine regulatory domain and alter local electrostatic potential to perturb intra- or intermolecular interactions required for kinase regulation<sup>5,9</sup>, rendering ALK2 constitutively active. Heterozygous mutations affecting the adjacent residue, Q207E, have been identified in phenotypic variant FOP<sup>10</sup>. The Q207E mutation and a well described man-made ALK2 mutation affecting the same residue, Q207D<sup>11</sup>, may exert similarly disruptive effects on the glycine-serine domain structure and to cause constitutive activation of ALK2. *In vivo*, transfer of the gene encoding ALK2<sup>Q207D</sup> but not wild-type ALK2 induces chondrogenic differentiation in chick embryos and promotes endochondral bone growth in cortical allografts<sup>12,13</sup>, consistent with potent osteogenic effects of constitutively activating ALK2 mutations.

To further explore the ability of constitutively active ALK2 to induce ectopic calcification, we took advantage of the availability of transgenic mice expressing an inducible ALK2<sup>Q207D</sup> (CAG-Z-EGFP-caALK2, or conditional caALK2). When the transgene is globally expressed during embryogenesis, mice are arrested at mid-gestation<sup>14</sup>, in contrast to individuals with FOP, who appear essentially normal at birth except for shortened great toes<sup>2</sup>. To circumvent the embryonic lethality of this transgene, we induced postnatal over-expression of ALK2<sup>Q207D</sup> in the left hindlimbs of mice with retro-popliteal injection of Ad.Cre ( $1 \times 10^8$  plaque-forming units (PFU)) on postnatal day 7 (P7). High-frequency, Cre-mediated recombination was evident by P11, with loss of nuclear  $\beta$ -galactosidase staining and gain of cytoplasmic GFP expression in myocytes, ligaments and vasculature only in the injected area (Fig. 1a). Mononuclear infiltrates and myofiber edema were apparent in the left gastrocnemius, soleus and hamstring muscles, consistent with myositis induced by intramuscular adenovirus injection<sup>15</sup>, whereas muscles of uninjected limbs appeared normal (Fig. 1a).

Conditional caALK2-expressing mice injected with Ad.Cre in the left hindlimb developed severely decreased mobility in the injected limb by P30, with loss of passive flexion in hip, knee and ankle joints when examined under anesthesia, whereas wild-type mice injected with

Ad.Cre retained normal posture and range of motion (Fig. 1b). By radiography and micro-computed tomography ( $\mu$ CT), bony calluses were evident in injected hindlimbs of conditional caALK2-expressing mice, circumferentially encasing the tibia and fibula (Fig. 1b,c). These calluses frequently fused with the pelvis and femur, rendering hip, knee and ankle joints immobile and extended and preventing the use of those limbs during locomotion (Supplementary Videos 1 and 2 online). At P30, the penetrance of heterotopic ossification and immobility associated with local induction of caALK2 by this technique was 100% (data not shown).

We recently identified a small-molecule inhibitor of BMP type I receptors, dorsomorphin (Fig. 2a), which selectively blocks ALK2, ALK3 and ALK6 activity<sup>16</sup>. We subsequently described the synthesis of potent and specific derivatives of dorsomorphin<sup>6</sup>. By reiteratively testing modifications of the parent molecule, we found that replacement of the pendent pyridine ring with a 4-quinolinyl group could improve potency that replacement of the 2-(1-piperidinyl) ethoxy group with piperazine improved metabolic stability and that, in general, modifications of the pyrazolo[1,5-a]pyrimidine core were not tolerated<sup>6</sup>. An optimized molecule, LDN-193189 (Fig. 2a), inhibited BMP4-mediated Smad1, Smad5 and Smad8 activation with greater potency than did dorsomorphin (half-maximal inhibitory concentration ( $IC_{50}$ ) = 5 nM versus 470 nM) while retaining 200-fold selectivity for BMP signaling versus transforming growth factor- $\beta$  (TGF- $\beta$ ) signaling ( $IC_{50}$  for TGF- $\beta$   $\geq$  1,000 nM; Fig. 2a-c). LDN-193189 efficiently inhibited transcriptional activity of the BMP type I receptors ALK2 and ALK3 ( $IC_{50}$  = 5 nM and 30 nM, respectively), with substantially weaker effects on activin and the TGF- $\beta$  type I receptors ALK4, ALK5 and ALK7 ( $IC_{50}$   $\geq$  500 nM, Supplementary Fig. 1 online) and increased selectivity for BMP signaling versus AMP-activated protein kinase, platelet-derived growth factor receptor and mitogen-activated protein kinase signaling pathways as compared to the parent compound<sup>16</sup> (Supplementary Fig. 2 online). LDN-193189 blocked the transcriptional activity induced by either constitutively active ALK2<sup>R206H</sup> or ALK2<sup>Q207D</sup> mutant proteins (Fig. 2d,e). These findings suggest that LDN-193189 might affect BMP-induced osteoblast differentiation. In fact, LDN-193189 inhibited the induction of alkaline phosphatase activity in C2C12 cells by BMP4 even when administered 12 h after BMP stimulation (Fig. 2f), indicating sustained BMP signaling activity is needed for osteogenic differentiation, as we have previously observed in vascular smooth muscle cells<sup>17</sup>.

To assess the impact of ALK2<sup>Q207D</sup> on BMP signaling, we isolated and cultured pulmonary artery smooth muscle cells (PASMCs) from conditional caALK2-expressing mice. Baseline phosphorylation of Smad1, Smad5 and Smad8 was increased in cells infected with Ad.Cre compared to those infected with Ad.GFP (Fig. 2g), consistent with increased basal BMP signaling after Cre-mediated induction of ALK2<sup>Q207D</sup>. PASMCs expressing ALK2<sup>Q207D</sup> also showed hyperresponsiveness to BMP ligands, consistent with observations in cells that express the mutant ALK2<sup>R206H</sup> protein<sup>18,19</sup>. Enhanced Smad1, Smad5 and Smad8 activation in cells expressing ALK2<sup>Q207D</sup> was effectively inhibited by treatment with LDN-193189 (Fig. 2g).

To determine the pharmacokinetics of LDN-193189, we measured its plasma concentration after administration of a single dose (3 mg kg<sup>-1</sup> intraperitoneally (i.p.)) in C57BL/6 mice. LDN-193189 remained at levels several fold higher than its *in vitro*  $IC_{50}$  for >8 h (Supplementary Fig. 3 online), suggesting sustained inhibition of BMP signaling might be obtained by bolus dosing. To assess the effect of ALK2 kinase inhibition on ectopic calcification *in vivo*, we injected conditional caALK2-transgenic and wild-type mice with Ad.Cre on P7 and then treated them with LDN-193189 (3 mg kg<sup>-1</sup> i.p. every 12 h) or with vehicle. Ad.Cre injection of conditional caALK2-transgenic mice led to mild calcifications surrounding the left tibia and fibula first visible at P13 on X-ray (Fig. 3a). By P15, these lesions were more prominent and extended to involve the distal femur (Fig. 3a). Lesions that effectively joined the hip, femur and tibia-fibula were present in all vehicle-treated, Ad.Cre-injected mice

by P30, progressing to fusion of the left hip, knee and ankle joints by P60 (Fig. 3a and Supplementary Fig. 4 online). Treatment of Ad.Cre-injected, caALK2-expressing mice with LDN-193189 prevented radiographic lesions at P15 in all mice examined (Fig. 3a). At P30, LDN-193189 prevented ectopic bone in approximately two-thirds of mice and attenuated lesions in the remainder, whereas at P60 LDN-193189 prevented ectopic bone in one-third of mice and attenuated lesions in the remainder (Supplementary Fig. 4). In contrast to vehicle-treated mice, LDN-193189-treated mice appeared to preserve knee and ankle joints at P30 and P60. Alizarin red and Alcian blue staining of vehicle-treated caALK2-expressing mice at P15 revealed ectopic bone encasing the tibia and fibula and increased cartilage formation in surrounding tissues (Fig. 3b,c). LDN-193189-treated mice showed no ectopic bone at P15 but did show enhanced cartilage formation in surrounding soft tissues compared to wild-type mice. Vehicle-treated, caALK2-expressing mice developed extensive ossification and fusion by P30 on  $\mu$ CT, whereas LDN-193189-treated, caALK2-expressing mice had small ectopic ossifications without joint fusion (Fig. 3d). Radiographic lesions in vehicle-treated mice correlated with abnormal hindlimb posture and decreased passive range of motion of hip, knee and ankle joints when the mice were examined under anesthesia, all of which were attenuated in LDN-193189-treated mice (Fig. 3e). A quantitative measure of passive range of motion in the ankle joint (Fig. 3f) appeared to be a sensitive marker of functional impairment (Fig. 3g), correlating with severe lesions found in vehicle-treated mutant mice while demonstrating significant rescue of function in LDN-193189-treated mice. In fact, LDN-193189-treated mice showed at least mildly impaired range of motion even in the absence of radiographically visible disease at P30, perhaps reflecting enhanced cartilage formation or early calcification (Fig. 3a–c,g). Consistent with this functional end point, vehicle-treated mice progressively lost use of the left hindlimb owing to joint fusion, whereas LDN-193189-treated mice retained use of the left hindlimb during ambulation at P15 and P30 (Supplementary Videos 3–6 online). Treatment of wild-type or mutant mice with LDN-193189 under this regimen did not cause weight loss or growth retardation (Supplementary Fig. 5 online), spontaneous fractures, decreased bone density (Fig. 3a) or lead to other skeletal, morphologic, hematological or behavioral abnormalities (data not shown).

Vehicle-treated, Ad.Cre-injected, caALK2-expressing mice showed increased amounts and nuclear accumulation of phosphorylated Smad1, Smad5 and Smad8 in the left gastrocnemius, soleus and hamstring muscles (Fig. 4a), whereas the uninjected right gastrocnemius had little detectable phosphorylated Smad1, Smad5 and Smad8. Consistent with enhanced Smad1, Smad5 and Smad8 signaling, *Id1* expression was more than threefold greater in the hindlimb muscles of Ad.Cre-injected, caALK2-expressing mice than in wild-type or uninjected mutant controls (Supplementary Fig. 6 online). Within Ad.Cre-injected muscle tissues, but not controls, a subset of myocyte-like cells was observed to express the osteogenic runt-related transcription factor-2 (Runx2; Fig. 4a). Treatment of conditional caALK2-transgenic mice with LDN-193189 did not have an impact on recombination efficiency, myocyte edema or inflammation, but did result in diminished phosphorylated Smad1, Smad5 and Smad8 and Runx2 staining in the left gastrocnemius (Fig. 4a). By P15, maturing endochondral bone, marked by alkaline phosphatase-positive osteoblasts, chondrocyte-like cells and marrow cells were evident in Ad.Cre-injected muscles of conditional caALK2-expressing mice (Fig. 4b). The hindlimbs of Ad.Cre-injected, conditional caALK2-expressing mice treated with LDN-193189 developed substantially less endochondral bone but retained evidence of inflammation and myocyte injury (Fig. 4b). Histological evolution of lesions in affected mice thus paralleled that of human intramuscular FOP lesions, showing myocyte injury and inflammatory infiltrate followed by elaboration of a chondrogenic matrix, osteoblast-mediated mineralization and maturation into endochondral bone<sup>20</sup>. This process of ectopic ossification, beginning with activation of Smad1, Smad5 and Smad8, was markedly attenuated by LDN-193189 treatment.

To test the sufficiency of transgenic expression of caALK2 for the development of ectopic bone, we used an alternate recombination strategy. We achieved global postnatal expression of ALK2<sup>Q207D</sup> by mating conditional caALK2–transgenic mice with CAGGS–CreER mice, which express a tamoxifen-inducible Cre recombinase ubiquitously<sup>21</sup>. Double-transgenic mice were injected with tamoxifen (0.5 mg i.p.) on P7, inducing high-frequency recombination of the gene segment encoding CAG–Z–EGFP–caALK2 throughout hindlimb muscle and vascular and connective tissues, as indicated by the loss of nuclear  $\beta$ -galactosidase staining (Fig. 4c). Muscle tissues undergoing recombination by this technique did not show edema or mononuclear cell infiltrates. In contrast to Ad.Cre-induced recombination, global postnatal overexpression of ALK2<sup>Q207D</sup> did not lead to detectable radiological ossification by P60 (Fig. 4d). When double-transgenic mice were injected with tamoxifen on P7 and injected with a control adenovirus (Ad.GFP,  $1 \times 10^8$  PFU, left popliteal fossa) on P8, mildly decreased left hindlimb range of motion and small ectopic calcifications appeared by P14 (Fig. 4e). These data suggest that expression of caALK2 is by itself insufficient to produce ectopic bone, and that inflammation or tissue injury from viral immunogenicity or cytotoxicity might be required for bone formation. To test this hypothesis, we treated conditional caALK2–expressing mice with dexamethasone ( $10 \text{ mg kg}^{-1} \text{ d}^{-1}$  i.p.) starting 1 d after Ad.Cre injection at P7 and assessed them for ectopic calcification. By P30, ectopic calcifications and immobility were markedly reduced in corticosteroid-treated mice compared with vehicle-treated mice (Fig. 4f,g). The impact of corticosteroid treatment suggests that inflammation and caALK2 expression are both required to form ectopic bone. Unlike LDN-193189 administration, dexamethasone administration was accompanied by toxicity, reflected by severely impaired weight gain during drug administration (Supplementary Figs. 5 and 7 online).

These studies provide a model of heterotopic ossification that recapitulates key features of human FOP, including the evolution of intramuscular endochondral bone and radiological and functional outcomes. Episodes of ectopic ossification in afflicted humans are frequently precipitated by viral prodromes and accompanying viral myositis<sup>22</sup>. Formation of ectopic bone in conditional caALK2–transgenic mice in conjunction with local adenovirus infection and the response to corticosteroid treatment support a similar relationship between ossification and inflammation in the mouse model as suggested in previous reports<sup>23,24</sup>. These studies confirm the role of dysregulated ALK2 kinase activity in the molecular pathogenesis of FOP<sup>19</sup> while demonstrating the potential of rational therapy mediated through inhibition of ALK2. Despite this promising result, it is worthwhile to note that before any human therapy can be considered using this approach, comprehensive and long-term toxicity studies in multiple species and further drug refinement and optimization will be necessary to ensure adequate safety of both the compound and chronic or intermittent inhibition of BMP signaling *in vivo*. Moreover, the ability of LDN-193189 to prevent ectopic ossification in conditional caALK2–transgenic mice was incomplete. It is possible that LDN-193189, in the manner it was administered, was insufficient to completely suppress activation of SMAD signaling. It is also conceivable that activation of SMAD-independent pathways, which were not blocked by dorsomorphin (ref. 16) and may not be inhibited by LDN-193189, can contribute to the ectopic ossification associated with caALK2 expression.

BMP signals have pivotal roles in vertebrate development, regulating gastrulation, patterning and organogenesis by specifying the fate of multipotent cells<sup>25</sup>. In contrast, the postnatal roles of BMP signals are most essential in the contexts of injury repair, inflammation or remodeling, in the skeleton as well as in connective and vascular tissues<sup>26,27</sup>. Given the apparent requirement for injury and enhanced BMP signaling for FOP lesions in humans and mice, it is possible that abnormal ossification results from diversion of an injury repair program toward bone formation, perhaps deviating the normal adaptive response of cells with regenerative potential. Understanding the cellular basis of endochondral bone formation in FOP could yield insights into the mechanism of heterotopic ossification of auto-immune, post-traumatic or

postsurgical etiologies and reveal how BMPs specify plasticity of mesenchyme-derived tissues in physiology and in disease.

## METHODS

### Chemical, protein and viral agents

We purchased dorsomorphin (Compound C, 6-[4-(2-piperidin-1-yl-ethoxy)phenyl]-3-pyridin-4-yl-pyrazolo[1,5-a]pyrimidine) from EMD Biosciences. We synthesized LDN-193189 (4-[6-(4-piperazin-1-ylphenyl)pyrazolo[1,5-a]pyrimidin-3-yl]quinoline) as previously described<sup>6</sup>, determined its purity (99.8%) by HPLC and confirmed its structure by <sup>1</sup>H-NMR and high-resolution mass spectrometry. The vehicle was 2% (wt/vol) (2-hydroxypropyl)- $\beta$ -cyclodextrin in PBS, pH 7.4. We purchased dexamethasone from Sigma. Recombinant human BMP4, platelet-derived growth factor-BB and TGF- $\beta$  were obtained from R&D Systems. We produced adenoviruses expressing GFP and Cre and quantified them by the plaque-titer method.

### Conditionally-expressed, constitutively-active ALK2–transgenic mice

The construction of mice expressing a single conditionally expressed allele of the gene encoding constitutively-active ALK2<sup>Q207D</sup> (CAG-Z-EGFP-caALK2) on a C57BL/6 background was previously described<sup>14</sup>. We obtained CAGGS-CreER mice, which express a tamoxifen-inducible Cre recombinase ubiquitously under the control of the cytomegalovirus immediate-early enhancer and the chicken  $\beta$ -actin promoter/enhancer<sup>20</sup>, from the Jackson Laboratory. All mouse experiments were approved by the Massachusetts General Hospital Subcommittee on Research Animal Care.

### Cell culture

We isolated PSMCs from wild-type and CAG-Z-EGFP-caALK2–transgenic mice as previously described<sup>28</sup> and cultured them in RPMI medium (Invitrogen) supplemented with 10% FBS. We induced recombination of PSMCs expressing conditional caALK2 *in vitro* by infecting with Ad.Cre (multiplicity of infection of 50) or Ad.GFP as a control and then culturing for 3 d and passaging. We cultured C2C12 myofibroblast cells (American Type Culture Collection) in DMEM (Invitrogen) supplemented with glutamine and 10% FBS. We preincubated cells with pharmacological inhibitors for 10 min and then exposed them to BMP4, TGF- $\beta$  or platelet-derived growth factor-BB ligands for 30 minutes at 37 °C.

### Immunoblot analysis of Smad1, Smad5 and Smad8 phosphorylation

We mechanically homogenized cell extracts in SDS-lysis buffer (62.5 mM Tris-HCl (pH 6.8), 2% SDS, 10% glycerol, 50 mM dithiothreitol and 0.01% bromophenol blue), separated the proteins by SDS-PAGE, immunoblotted with polyclonal antibodies specific for phosphorylated Smad1, Smad5 and Smad8, phosphorylated Smad2 (Cell Signaling Technology) or rabbit monoclonal antibodies specific for Smad1 (Epitomics) or Smad2 (Cell Signaling), and visualized the immunoreactive proteins with ECL Plus (GE Healthcare).

### Alkaline phosphatase activity

We seeded C2C12 cells into 96-well plates at 2,000 cells per well in DMEM supplemented with 2% FBS. We treated the wells in quadruplicate with BMP ligands and LDN-193189 or vehicle. We collected the cells after 6 d in culture in 50  $\mu$ l Tris-buffered saline and 1% Triton X-100. We added the lysates to *p*-nitro-phenylphosphate reagent in 96-well plates (Sigma) for 1 h and then evaluated alkaline phosphatase activity (absorbance at 405 nm). We measured cell viability and quantity by Cell Titer Aqueous One (absorbance at 490 nm, Promega), using replicate wells treated identically to those used for alkaline phosphatase measurements.

## Visualization of skeletal mineralization

We fixed soft tissues and bone and stained them with Alizarin red and Alcian blue as previously described<sup>29</sup>.

## Radiography

For plain film radiography, we anesthetized the mice with ketamine and xylazine and then immobilized them and X-rayed them. For three-dimensional images, we killed the mice and analyzed them with a desktop microtomographic imaging system ( $\mu$ CT40, Scanco Medical AG) equipped with a 10-mm focal spot microfocus X-ray tube. We acquired transverse CT slices of the lower pelvis and hindlimbs with a 12- $\mu$ m isotropic voxel size. We reconstructed, filtered and thresholded the images with a specimen-specific threshold.

## Histology

We killed mice and fixed their limbs in 0.5% paraformaldehyde in PBS overnight and then decalcified them in 14% EDTA disodium salt solution with daily changes for 3 d. We incubated the limbs overnight in 30% sucrose with PBS, embedded them in optimal cutting-temperature medium and prepared 12- $\mu$ m sections with the Cryo-Jane system (Instrumedics). We stained sections for  $\beta$ -galactosidase or alkaline phosphatase activity (X-Gal and BM purple stains, respectively, Roche), and/or with hematoxylin or eosin counter-stains. For immunofluorescence, we post-fixed sections in cold methanol to disrupt GFP fluorescence and incubated them with polyclonal antibodies specific for phosphorylated Smad1, Smad5 and Smad8 (1:100, Cell Signaling) or Runx2 (M-70, 1:200, Santa Cruz Biotechnology), followed by Alexa Fluor 488-labeled goat Fab specific for rabbit IgG (Invitrogen).

## Id1 and plasminogen activator inhibitor-1 promoter luciferase reporter assays

We transiently transfected mouse PASCs grown to 50% confluence in six-well plates with 0.3  $\mu$ g *Id1* promoter luciferase reporter construct (BRE-Luc30, kindly provided by P. ten Dijke) in combination with 0.6  $\mu$ g of plasmid expressing constitutively active forms of BMP type I receptors (caALK2, caALK3 or caALK631, kindly provided by K. Miyazono), using Fugene6 (Roche). To assess activin and TGF- $\beta$  type I receptor function, we transiently transfected PASCs with 0.3  $\mu$ g *Pai1* (plasminogen activator inhibitor-1) promoter luciferase reporter construct (CAGA-Luc32, provided by P. ten Dijke) in combination with 0.6  $\mu$ g of plasmid expressing constitutively active forms of type I receptors (caALK4, caALK5 and caALK733, provided by K. Miyazono). For both reporter plasmids, we used 0.2  $\mu$ g of pRL-TK *Renilla* luciferase (Promega) to control for transfection efficiency. We incubated PASCs with LDN-193189 (2 nM–32  $\mu$ M) or vehicle starting 1 h after transfection. We harvested cell extracts and quantified relative promoter activity by the ratio of firefly to *Renilla* luciferase activity with the dual luciferase assay kit (Promega).

## Range of motion analyses

To quantify impaired mobility via passive range of motion, we anesthetized transgenic and control mice and assessed them for the ability to passively dorsiflex the left ankle joint. Scores were assessed by two independent observers blinded to genotype and treatment. The observers scored the minimum angle formed by the ankle and the tibia with passive dorsiflexion under light manual pressure as follows: 0, normal flexion with a minimal angle of  $< 20^\circ$ ; 1, mildly impaired flexion with a minimal angle of  $\geq 20^\circ$  but  $< 90^\circ$ ; 2, moderately impaired flexion with a minimal angle of  $\geq 90^\circ$  but  $< 135^\circ$ ; and 3, severely impaired flexion with a minimal angle of  $\geq 135^\circ$  (depicted in Fig. 3f).

## Statistical analyses

We measured the statistical significance of compared measurements with the Student's two-tailed *t*-test.

## Supplementary Material

Refer to Web version on PubMed Central for supplementary material.

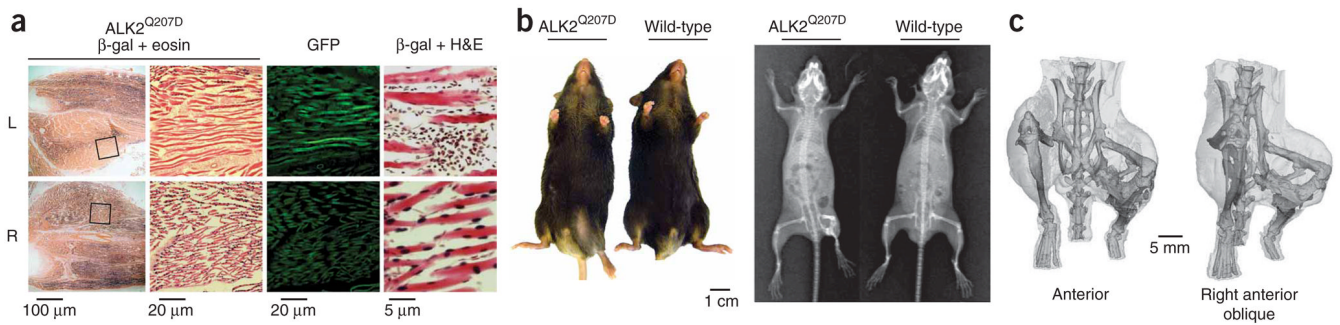
## Acknowledgments

We thank P. ten Dijke (Leiden University Medical Center) for providing BRE-Luc and CAGA-Luc and K. Miyazono (University of Tokyo) for providing caALK2, caALK3, caALK4, caALK5, caALK6 and caALK7. We are grateful to H. Beppu, E. Schipani, H. Kronenberg, A. Wagers, J. Groppe, W. Zapol and F. Kaplan for insightful discussions and technical expertise, A. Graveline and D. Panus for technical assistance and E. Buys for technical expertise. This work was supported by US National Institutes of Health grants HL079943 (P.B.Y.) and HL074352 (K.D.B.), the US National Institute of Environmental Health Sciences Intramural Research Program grant ES071003-10 (Y.M.) and Partners Healthcare. This work was also supported by a Howard Hughes Medical Institute Early Career Award (P.B.Y.), a Pulmonary Hypertension Association Mentored Clinical Scientist Award (P.B.Y.), a grant from the GlaxoSmithKline Research & Education Foundation for Cardiovascular Disease (P.B.Y.) and a Developmental Grant from the Center for Research in Fibrodysplasia Ossificans Progressiva and Related Disorders at the University of Pennsylvania (C.C.H.).

## References

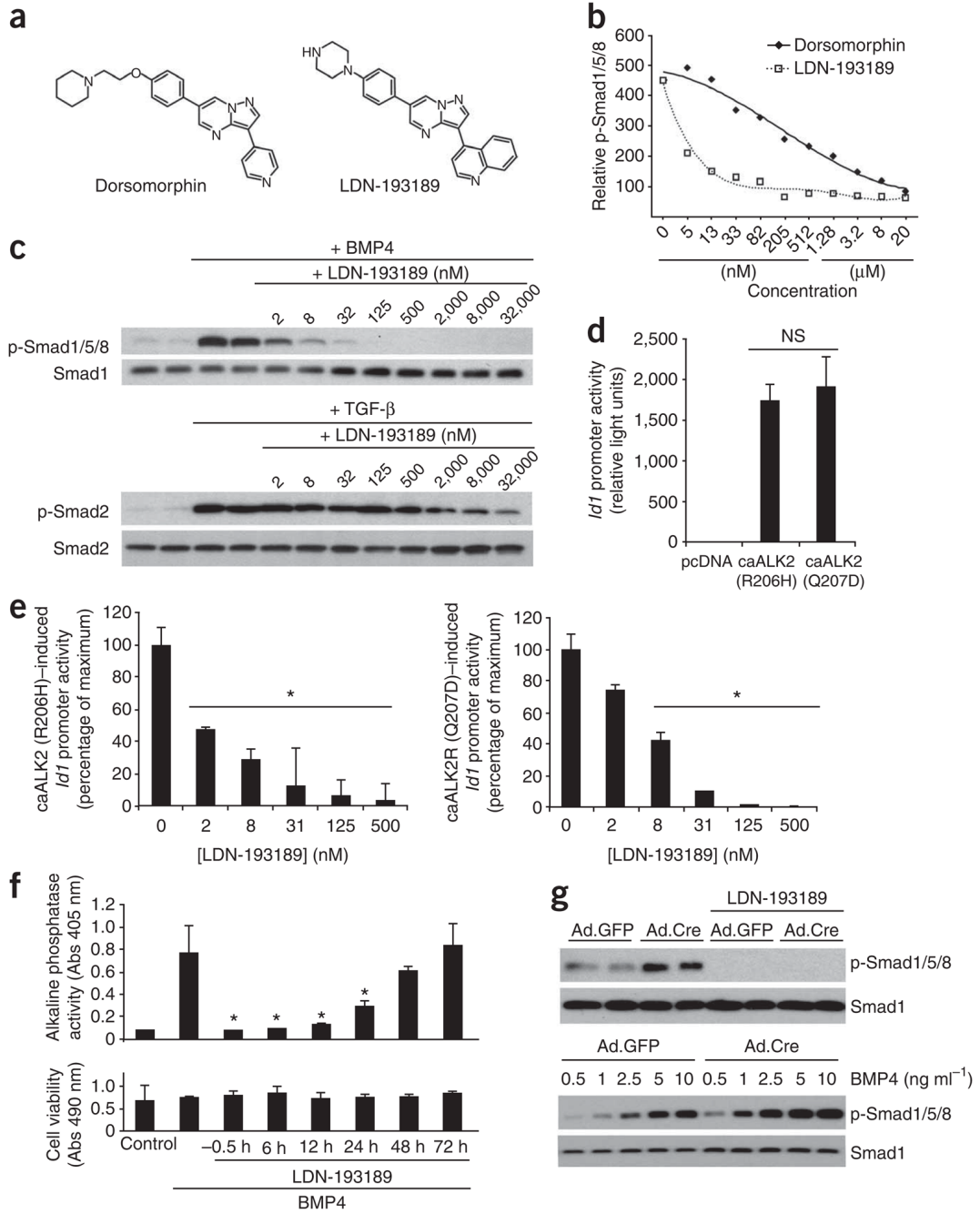
1. Shore EM, Kaplan FS. Insights from a rare genetic disorder of extra-skeletal bone formation, fibrodysplasia ossificans progressiva (FOP). *Bone* 2008;43:427–433. [PubMed: 18590993]
2. Buyse G, Silberstein J, Goemans N, Casaer P. Fibrodysplasia ossificans progressiva: still turning into wood after 300 years? *Eur J Pediatr* 1995;154:694–699. [PubMed: 8582418]
3. Kaplan FS, Glaser DL, Pignolo RJ, Shore EM. A new era for fibrodysplasia ossificans progressiva: a druggable target for the second skeleton. *Expert Opin Biol Ther* 2007;7:705–712. [PubMed: 17477807]
4. Kaplan FS, et al. Fibrodysplasia ossificans progressiva. *Best Pract Res Clin Rheumatol* 2008;22:191–205. [PubMed: 18328989]
5. Shore EM, et al. A recurrent mutation in the BMP type I receptor ACVR1 causes inherited and sporadic fibrodysplasia ossificans progressiva. *Nat Genet* 2006;38:525–527. [PubMed: 16642017]
6. Cuny GD, et al. Structure-activity relationship study of bone morphogenetic protein (BMP) signaling inhibitors. *Bioorg Med Chem Lett* 2008;18:4388–4392. [PubMed: 18621530]
7. Tsuchida K, Mathews LS, Vale WW. Cloning and characterization of a transmembrane serine kinase that acts as an activin type I receptor. *Proc Natl Acad Sci USA* 1993;90:11242–11246. [PubMed: 8248234]
8. Miyazono K, Maeda S, Imamura T. BMP receptor signaling: Transcriptional targets, regulation of signals, and signaling cross-talk. *Cytokine Growth Factor Rev* 2005;16:251–263. [PubMed: 15871923]
9. Groppe JC, Shore EM, Kaplan FS. Functional modeling of the ACVR1 (R206H) mutation in FOP. *Clin Orthop Relat Res* 2007;462:87–92. [PubMed: 17572636]
10. Shore EM, Xu M, Connor JM, Kaplan FS. Mutations in the BMP type I receptor ACVR1 in patients with fibrodysplasia ossificans progressiva (FOP). *J Bone Miner Res* 2006;21:S75.
11. Macias-Silva M, Hoodless PA, Tang SJ, Buchwald M, Wrana JL. Specific activation of Smad1 signaling pathways by the BMP7 type I receptor, ALK2. *J Biol Chem* 1998;273:25628–25636. [PubMed: 9748228]
12. Zhang D, et al. ALK2 functions as a BMP type I receptor and induces Indian hedgehog in chondrocytes during skeletal development. *J Bone Miner Res* 2003;18:1593–1604. [PubMed: 12968668]
13. Koefoed M, et al. Biological effects of rAAV-caAlk2 coating on structural allograft healing. *Mol Ther* 2005;12:212–218. [PubMed: 16043092]

14. Fukuda T, et al. Generation of a mouse with conditionally activated signaling through the BMP receptor, ALK2. *Genesis* 2006;44:159–167. [PubMed: 16604518]
15. Waheed I, et al. Factors associated with induced chronic inflammation in mdx skeletal muscle cause posttranslational stabilization and augmentation of extrasynaptic sarcolemmal utrophin. *Hum Gene Ther* 2005;16:489–501. [PubMed: 15871680]
16. Yu PB, et al. Dorsomorphin inhibits BMP signals required for embryogenesis and iron metabolism. *Nat Chem Biol* 2008;4:33–41. [PubMed: 18026094]
17. Yu PB, et al. Bone morphogenetic protein (BMP) type II receptor is required for BMP-mediated growth arrest and differentiation in pulmonary artery smooth muscle cells. *J Biol Chem* 2008;283:3877–3888. [PubMed: 18042551]
18. Billings PC, et al. Dysregulated BMP signaling and enhanced osteogenic differentiation of connective tissue progenitor cells from patients with fibrodysplasia ossificans progressiva (FOP). *J Bone Miner Res* 2008;23:305–313. [PubMed: 17967130]
19. Fukuda T, et al. Constitutively activated ALK2 and increased smad1/5 cooperatively induce BMP signaling in fibrodysplasia ossificans progressiva. *J Biol Chem*. August 6;2008 published online. 10.1074/jbc.M801681200
20. Hegyi L, et al. Stromal cells of fibrodysplasia ossificans progressiva lesions express smooth muscle lineage markers and the osteogenic transcription factor Runx2/Cbfa-1: clues to a vascular origin of heterotopic ossification? *J Pathol* 2003;201:141–148. [PubMed: 12950027]
21. Hayashi S, McMahon AP. Efficient recombination in diverse tissues by a tamoxifen-inducible form of Cre: a tool for temporally regulated gene activation/inactivation in the mouse. *Dev Biol* 2002;244:305–318. [PubMed: 11944939]
22. Scarlett RF, et al. Influenza-like viral illnesses and flare-ups of fibrodysplasia ossificans progressiva. *Clin Orthop Relat Res* 2004;275–279. [PubMed: 15232462]
23. Kaplan FS, et al. Hematopoietic stem-cell contribution to ectopic skeletogenesis. *J Bone Joint Surg Am* 2007;89:347–357. [PubMed: 17272450]
24. Pignolo RJ, Suda RK, Kaplan FS. The fibrodysplasia ossificans progressiva lesion. *Clin Rev Bone Miner Metab* 2005;5:195–200.
25. Zhao GQ. Consequences of knocking out BMP signaling in the mouse. *Genesis* 2003;35:43–56. [PubMed: 12481298]
26. Tsuji K, et al. BMP2 activity, although dispensable for bone formation, is required for the initiation of fracture healing. *Nat Genet* 2006;38:1424–1429. [PubMed: 17099713]
27. Corriere MA, et al. Endothelial Bmp4 is induced during arterial remodeling: effects on smooth muscle cell migration and proliferation. *J Surg Res* 2008;145:142–149. [PubMed: 17706674]
28. Yu PB, Beppu H, Kawai N, Li E, Bloch KD. Bone morphogenetic protein (BMP) type II receptor deletion reveals BMP ligand-specific gain of signaling in pulmonary artery smooth muscle cells. *J Biol Chem* 2005;280:24443–24450. [PubMed: 15883158]
29. Komori T, et al. Targeted disruption of *Cbfa1* results in a complete lack of bone formation owing to maturational arrest of osteoblasts. *Cell* 1997;89:755–764. [PubMed: 9182763]
30. Korchynskiy O, ten Dijke P. Identification and functional characterization of distinct critically important bone morphogenetic protein-specific response elements in the *Id1* promoter. *J Biol Chem* 2002;277:4883–4891. [PubMed: 11729207]
31. Fujii M, et al. Roles of bone morphogenetic protein type I receptors and Smad proteins in osteoblast and chondroblast differentiation. *Mol Biol Cell* 1999;10:3801–3813. [PubMed: 10564272]
32. Dennler S, et al. Direct binding of Smad3 and Smad4 to critical TGF  $\beta$ -inducible elements in the promoter of human plasminogen activator inhibitor-type 1 gene. *EMBO J* 1998;17:3091–3100. [PubMed: 9606191]
33. Shimizu A, et al. Identification of receptors and Smad proteins involved in activin signalling in a human epidermal keratinocyte cell line. *Genes Cells* 1998;3:125–134. [PubMed: 9605406]



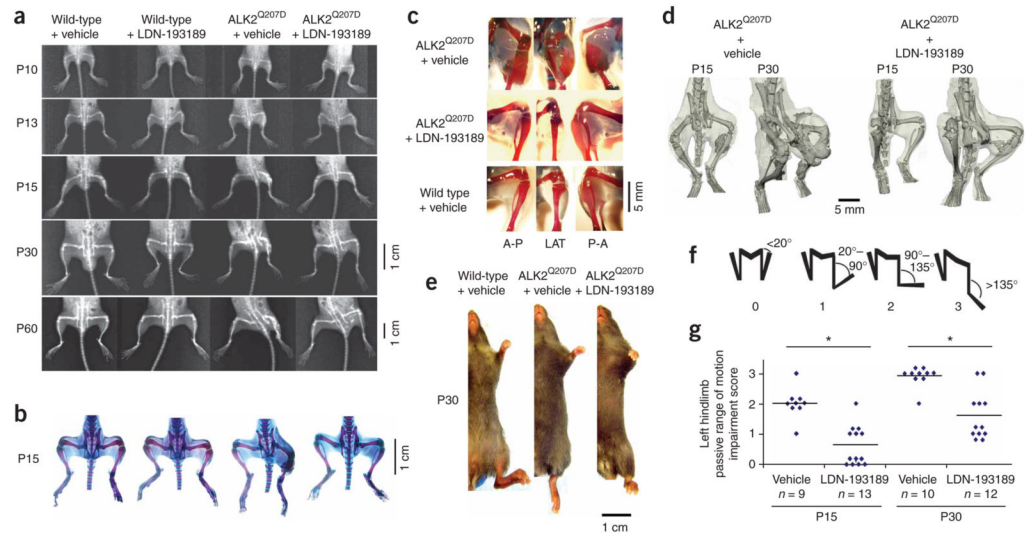
**Figure 1.**

Mouse model of FOP. **(a)** Staining of muscle sections from Ad.Cre-injected conditional caALK2-expressing (ALK<sup>Q207D</sup>) mice. The injection done at P7 induced recombination in myocytes of the left (L) gastrocnemius and soleus muscles at P11, as evidenced by loss of nuclear β-galactosidase (β-gal) staining and gain of GFP expression. Squares indicate areas of low magnification examined at higher magnification to the right. H&E staining reveals mononuclear cell infiltrates and myocyte edema in tissues undergoing recombination, but not in uninjected right (R) hindlimb muscles. **(b)** Left hindlimb postural abnormalities were observed grossly (left) at P30 in the Ad.Cre-injected left hindlimbs of conditional caALK2 mice, but not in Ad.Cre-injected wild-type mice. The X-ray image (right) shows Ad.Cre-induced ectopic calcifications involving the left gastrocnemius, soleus and hamstring muscles of conditional caALK2 mice at P30. **(c)** Three-dimensional reconstructed images from μCT cross-sections of an Ad.Cre-injected, conditional caALK2-expressing mouse on P30 showing intramuscular ectopic bone within the left gastrocnemius, soleus, tibialis and hamstring muscles (rendered in light gray) fusing with the pelvis and proximal femur.

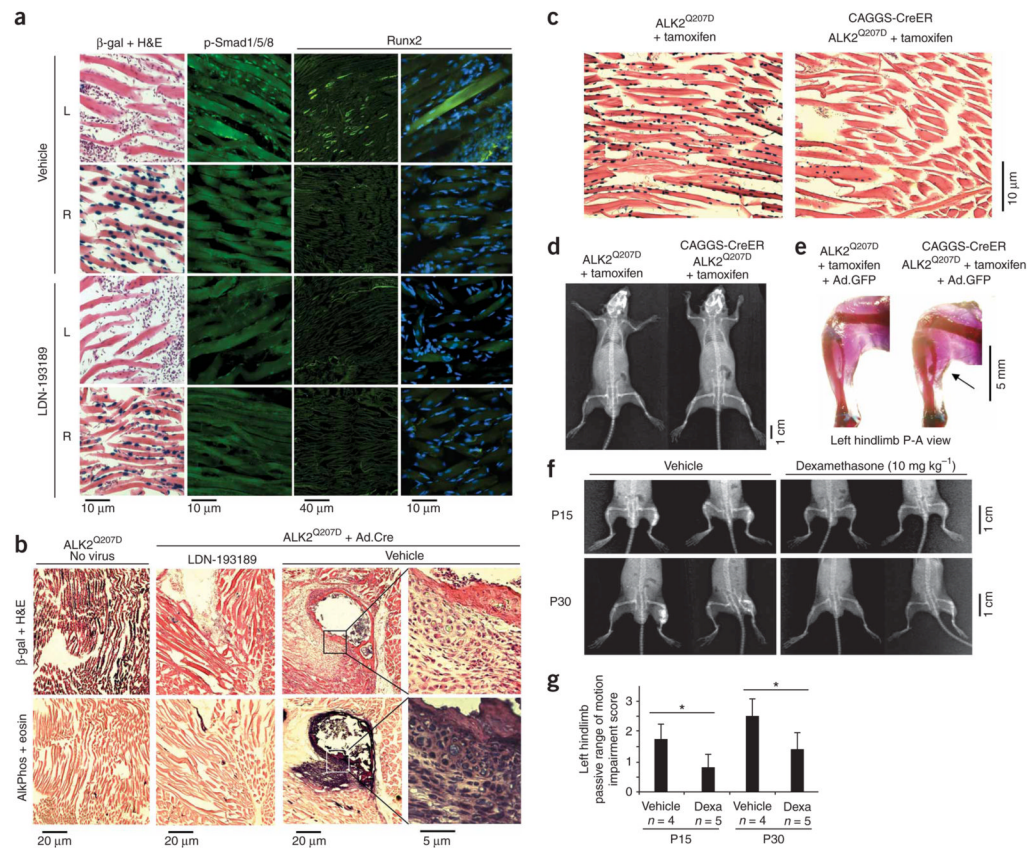


**Figure 2.** Effect of LDN-193189 on BMP signaling and function. **(a)** Structures of dorsomorphin and LDN-193189. **(b)** Quantitative immunoblotting of PASCs showing differential effects of dorsomorphin or LDN-193189 on BMP4-induced ( $10 \text{ ng ml}^{-1}$ ) phosphorylation of Smad1, Smad5 and Smad8 (p-Smad1/5/8), with  $IC_{50}$  values of  $\sim 400 \text{ nM}$  and  $\sim 5 \text{ nM}$ , respectively. **(c)** Immunoblot of PASCs treated with LDN-193189 showing differential inhibition of BMP4 ( $10 \text{ ng ml}^{-1}$ ) or TGF- $\beta$  ( $0.5 \text{ ng ml}^{-1}$ ) signaling ( $IC_{50} \sim 5 \text{ nM}$  and  $\geq 1 \mu\text{M}$ , respectively). **(d)** *Id1* promoter activity induced by transient transfection of COS cells with ALK2<sup>R206H</sup> or ALK2<sup>Q207D</sup>. *Id1* promoter activity (BRE-Luc) was increased by 250- to 300-fold over control plasmid (pcDNA,  $n = 3$  measurements, mean  $\pm$  s.d., NS, no significant difference). **(e)** Impact

of LDN-193189 on the transcriptional activities of caALK2<sup>R206H</sup> and caALK2<sup>Q207D</sup> mutants, expressed as percentage of full *Id1* promoter activity ( $n = 3$  measurements, mean  $\pm$  s.d.,  $*P < 0.05$  versus untreated). (f) Impact of LDN-193189 (100 nM) on BMP4-induced (10 ng ml<sup>-1</sup>) osteoblast differentiation of C2C12 cells at various intervals before and after BMP4 treatment ( $n = 6$  measurements, mean  $\pm$  s.d.,  $*P < 0.01$  versus BMP4 treatment alone) and on cell viability (bottom panel). (g) Top, immunoblot for p-Smad1/5/8 and total Smad1 in PSMCs expressing the conditional caALK2<sup>Q207D</sup> transgene after infection with Ad.Cre or Ad.GFP showing the impact of pretreatment with LDN-193189 (100 nM). Bottom, immunoblot for phosphorylated Smad1/5/8 and total Smad1 in Ad.GFP- or Ad.Cre-infected PSMCs treated with BMP4 at varying concentrations.



**Figure 3.** Impact of LDN-193189 on ectopic ossification *in vivo*. **(a)** Conditional caALK2–expressing mice receiving vehicle after Ad.Cre injection on P7 developed radiographic disease at P13, progressing to fusion of left hindlimb joints by P30–P60, whereas treatment with LDN-193189 diminished ectopic bone formation and preserved joint spaces over the same interval without inducing fractures, osteopenia or skeletal abnormalities ( $n = 3–5$  mice per treatment group; data are representative of six independent experiments). **(b,c)** Alizarin red and Alcian blue staining of mice at P15 showing ectopic calcifications encasing the left tibia and fibula in vehicle-treated conditional caALK2–expressing mice, but not in LDN-193189–treated mice. Higher magnification images are shown in **c**. Ectopic bone or cartilage are absent in the wild-type hindlimb. A-P, anterior-posterior; LAT, lateral; P-A, posterior-anterior. **(d)**  $\mu$ CT imaging showing attenuated ectopic calcification in LDN-193189–treated mice as compared to vehicle-treated mice at P15 and P30. **(e)** Fixed extension of left hip, knee and ankle joints, as evident in anesthetized and flaccid Ad.Cre-injected conditional caALK2–mutant mice at P30. The extension is attenuated in LDN-193189–treated mice. **(f)** Passive range of motion impairment score, as assessed by the minimum angle formed by the ankle and tibia with passive dorsoflexion. **(g)** Impact of vehicle and LDN-193189 treatment upon passive range of motion impairment in Ad.Cre-injected conditional caALK2–mutant mice at P15 and P30 ( $n$  as indicated, bars represent mean,  $*P < 0.001$ ).

**Figure 4.**

Impact of pharmacologic inhibition of BMP signaling and inflammation in the mouse FOP model. **(a)** Immunofluorescence showing enhanced nuclear p-Smad1/5/8 and expression of Runx2 in a number of recombined ( $\beta$ -gal–negative) myocytes from left (L) hindlimb muscles of Ad.Cre–injected, conditional caALK2–mutant mice at P11 (with DAPI counterstain in blue, right). Both are diminished in LDN-193189–treated mice. Uninjected right(R)–hindlimbs are shown as controls. **(b)** Histological evidence of intramuscular endochondral bone, as shown by alkaline phosphatase staining (AlkPhos) of osteoblasts, chondrocytes, matrix and marrow cells in recombined tissues of vehicle–treated, Ad.Cre–injected, caALK2–transgenic mice at P30. The staining is diminished and absent in LDN-193189–treated and uninfected mice, respectively (higher magnification, right panels). **(c)** High–frequency recombination evidenced by loss of  $\beta$ -gal staining in muscle, vascular and connective tissues of tamoxifen–treated, CAGGS–CreER:CAG–Z–EGFP–caALK2 mice but not single–transgenic CAG–Z–EGFP–caALK2 mice at P30. **(d)** Plain radiographs of tamoxifen–treated double– and single–transgenic mice at P60 show absence of ectopic calcification. **(e)** Alizarin red and Alcian blue staining revealing ectopic calcification in tamoxifen–treated, Ad.GFP–injected double–transgenic but not single–transgenic mice at P14. **(f)** Impact of dexamethasone treatment (10 mg kg<sup>-1</sup> daily) upon radiographic ossifications in Ad.Cre–injected, conditional caALK2–expressing mice at P15 and P30, as compared to vehicle treatment. **(g)** Impact of dexamethasone treatment upon impairment of passive range of motion (ankle flexion) in Ad.Cre–injected, conditional caALK2–expressing mice at P15 and P30 (data are representative of three independent experiments,  $n$  as indicated; values are mean  $\pm$  s.d.,  $*P < 0.05$ ).